Concatenated dynamical decoupling with virtual pulses

Gonzalo A. Álvarez,* Alexandre M. Souza,† and Dieter Suter‡
Fakultät Physik, Technische Universität Dortmund, Dortmund, Germany.

The loss of quantum information due to interaction with external degrees of freedom, which is known as decoherence, remains one of the main obstacles for large-scale implementations of quantum computing. Accordingly, different measures are being explored for reducing its effect. One of them is dynamical decoupling (DD) which offers a practical solution because it only requires the application of control pulses to the system qubits. Starting from basic DD sequences, more sophisticated schemes were developed that eliminate higher-order terms of the system-environment interaction and are also more robust against experimental imperfections. A particularly successful scheme, called concatenated DD (CDD), gives a recipe for generating higher order sequences by inserting lower order sequences into the delays of a generating sequence. Here, we show how this scheme can be improved further by converting some of the pulses to virtual (and thus ideal) pulses. The resulting scheme, called vCDD, has lower power deposition and is more robust against pulse imperfections than the original CDD scheme.

PACS numbers: 03.65.Yz, 76.60.Es, 76.60.Lz, 03.67.Pp

I. INTRODUCTION

Quantum information processing has acquired a huge interest over the last decades. It can potentially solve many problems qualitatively faster than classical information processing. The quest to implement this scheme has led to a lot of progress on quantum control methodologies and technologies (see, e.g., [1]). The main obstacle for its implementation is the sensitivity of quantum systems to interactions with external degrees of fredom that destroy or modify the information to be processed in an uncontrolled way [2]. A number of techniques are currently being developed to make reliable quantum computing possible in the presence of environmental noise. A relatively simple technique is dynamical decoupling (DD) [3–15], which uses sequences of control pulses applied to the system qubits. This technique does not require any overhead in terms of ancilla qubits and requires no additional controls over those that are already needed for information processing. This field has seen significant progress over the last years, and the concept has been demonstrated on a number of different systems [11, 16–32].

In the limit of infinitely many ideal refocusing pulses, the DD scheme allows one to completely eliminate the decoherence due to the environmental noise. However, in any real physical implementation, the control pulses necessarily have finite duration and unavoidable imperfections. This leads to a significant reduction of the DD performance, and the effect of a real pulse sequence on the system can actually reduce the fidelity instead of improving it [20, 33–40]. These recent results have shown that efficient DD schemes must be able to preserve the system fidelity even in the presence of non-ideal control fields [20, 24, 26, 35, 39, 41, 42].

One strategy that was shown to be robust against imperfections is a technique called concatenated dynamical decoupling (CDD), which is based on a building block sequence that is concatenated recursively [5, 33]. This procedure improves the DD performance with the concatenation order. If the delays between the pulses can be reduced indefinitely, CDD was demonstrated to improve its performance with the concatenation order. However if the delays between the pulses are constrained or the pulses have errors, it was predicted [33] and experimentally demonstrated [20] that an optimal concatenation order exists, and beyond that the DD performance will not improve or even deteriorate.

To increase the concatenation order, the procedure inserts the lower-order CDD sequence within the delays of the building block sequence. If the pulses have imperfections and the buiding block sequence compensates partially their effects at the end of the cycle, the CDD sequence will also compensate them at the end of the complete sequence. However, if the average delay between pulses is kept fixed [20, 25, 26], the duration of the CDD cycle increases exponentially with the CDD order. The compensation of the pulse imperfections only occurs at the end of the cycle. If the cycle time exceeds the correlation time of the environmental fluctuations, this error compensation becomes inefficient and the DD performance decreases.

In this article, we present a new approach to the CDD scheme that does not require waiting for the end of the cycle to compensate the pulse imperfections. Instead, they are always compensated over the duration of the lowest order cycle. This is done by introducing virtual pulses for the building block sequence to generate the higher CDD order. Being virtual, *i.e.*, mathematical operations, these pulses are ideal and do not introduce any imperfections. As a result, this new method is more robust against pulse imperfections and improves the DD performance signifi-

*gonzalo.alvarez@tu-dortmund.de
†alexandre@e3.physik.uni-dortmund.de
‡Dieter.Suter@tu-dortmund.de

cantly. Here, we give a theoretical analysis of this scheme and show experimentally that it performs better than the standard CDD method when applied to a single qubit interacting with a pure dephasing environment - a typical situation for many QIP implementations [1].

II. THE SYSTEM

We consider a single qubit $\hat{S}$ as the system that is coupled to a bath. The free evolution Hamiltonian is

$$\widehat{\mathcal{H}}_f = \widehat{\mathcal{H}}_{SE} + \widehat{\mathcal{H}}_E, \tag{1}$$

in a suitable rotating frame of reference that is on resonance with the system qubit [43]. $\widehat{\mathcal{H}}_E$ is the environment Hamiltonian and

$$\widehat{\mathcal{H}}_{SE} = \sum_{\beta} \left(b_z^{\beta} \hat{E}_z^{\beta} \hat{S}_z + b_y^{\beta} \hat{E}_y^{\beta} \hat{S}_y + b_x^{\beta} \hat{E}_x^{\beta} \hat{S}_x \right) \tag{2}$$

is a general system-environment (SE) interaction. The operators $\hat{E}_u^{\beta}$ are environment operators and b_u^{β} the SE coupling strengths. The index β runs over all modes of the environment. Dephasing effects come from the interaction that affects the z component of the spin-system operator, and spin-flips and/or polarization damping are produced trough the x and/or y operators. We will discuss our method in a general SE interaction context, but the experimental results were performed on a spin-system coupled with a spin-bath. The SE interaction is given by a heteronuclear spin-spin interaction that effects a pure dephasing. In general, this type of interaction is naturally encountered in a wide range of solid-state spin systems, for example in nuclear mangetic resonance (NMR) [20, 25, 44, 45], electron spins in diamonds [24], electron spins in quantum dots [46], donors in silicon [47], etc. In other cases, when the system and environment have similar energies, the SE interaction can include terms along the x, y and z axis.

III. CDD WITH REAL AND VIRTUAL PULSES

A. CDD

Concatenated DD (CDD) is a scheme for improving the efficiency of a DD sequence [5, 33] by recursively concatenating lower order sequences CDD_{n-1} into a higher-order sequence CDD_n by inserting CDD_{n-1} blocks into the delays of a generating sequence

$$\mathrm{CDD}_n = C_n = C_{n-1}\hat{X}C_{n-1}\hat{Y}C_{n-1}\hat{X}C_{n-1}\hat{Y}, \tag{3}$$

where $C_0 = \tau$ is a free evolution period and $\hat{X}$ and $\hat{Y}$ are π-pulses of the generating sequence. $\mathrm{CDD}_1 = C_1 = XY4$ consists of four rotations around the x- and y-axes. Its pulse sequences is given by $XY4 = \tau$-$\hat{X}$-τ-$\hat{Y}$-τ-$\hat{X}$-τ-$\hat{Y}$. This sequence can decouple SE interactions that include all three components of the system spin operator [3] and it mitigates the effect of pulse errors compared to the older CPMG sequence consisting of identical pulses [48]. This can be understood by considering that pulse imperfections convert an Ising-type SE interaction into an effective general SE interaction [20, 33, 35], which can be partially eliminated by the $XY4$ sequence. In the QIP community, the $XY4$ sequence is usually referred to as periodic dynamical decoupling (PDD). Alternatively, we proposed to use the time symmetric version of $XY4$ [48] in the CDD protocol because the resulting CDD(s) sequences are are more efficient at supressing decoherence and pulse error effects [26, 35, 41]. These symmetric sequences can be written as [26, 41, 48] $XY4(\mathrm{s}) = \tau/2$-$\hat{X}$-τ-$\hat{Y}$-τ-$\hat{X}$-τ-$\hat{Y}$-$\tau/2$ and

$$\begin{aligned} &\mathrm{CDD}(\mathrm{s})_n = C(s)_n = \\ &= \sqrt{C(s)_{n-1}}\hat{X}C(s)_{n-1}\hat{Y}C(s)_{n-1}\hat{X}C(s)_{n-1}\hat{Y}\sqrt{C(s)_{n-1}}. \end{aligned} \tag{4}$$

The square root $\sqrt{C(s)_n}$ represents half of the cycle. Each level of concatenation reduces the norm of the first non-vanishing term of the Magnus expansion of the previous level, provided that the norm was small enough to begin with [5, 33]. This reduction comes at the expense of an increase of the cycle time by a factor of four. The average Hamiltonian can be calculated in the toggling frame. If the pulses generate ideal π-rotations, this can be seen as a sign change of different terms of the SE interaction (2). The top panel of Fig. 1 shows the CDD_2 scheme and it shows the sign changes of the different terms of the SE interaction in the toggling frame. The parameters f_u with $u = x, y, z$ represent the signs of the terms of Eq. (2) that are proportional to $\hat{S}_x$, $\hat{S}_y$ and $\hat{S}_z$, respectively, in the toggling frame.

B. Effect of pulse imperfections in CDD

Since the precision of any real pulse is finite, they generate an evolution that differs from the ideal one. If many pulses are applied in sequence, these errors can accumulate and seriously reduce the fidelity of the evolution [20, 26, 35–38], unless the sequence of operations is designed in such a way that the errors from different pulses compensate each other [26, 35]. One kind of error of non-ideal control pulses is their finite duration, which implies a minimum achievable cycle time. The effects introduced by finite pulse lengths have been considered in different theoretical works [4, 33, 34]. These works predict that high order CDD sequences can lose their advantages when the delays between pulses or pulse length are strongly constrained. This is because the fundamental frequency $2\pi/\tau_c$, where τ_c is the period of the toggling frame function $f(t)$, is lower for the longer cycle [25]. The efficiency of all DD sequences is reduced if the noise contains frequency components at the resonance frequencies of their filter function [49]. This was demonstrated for

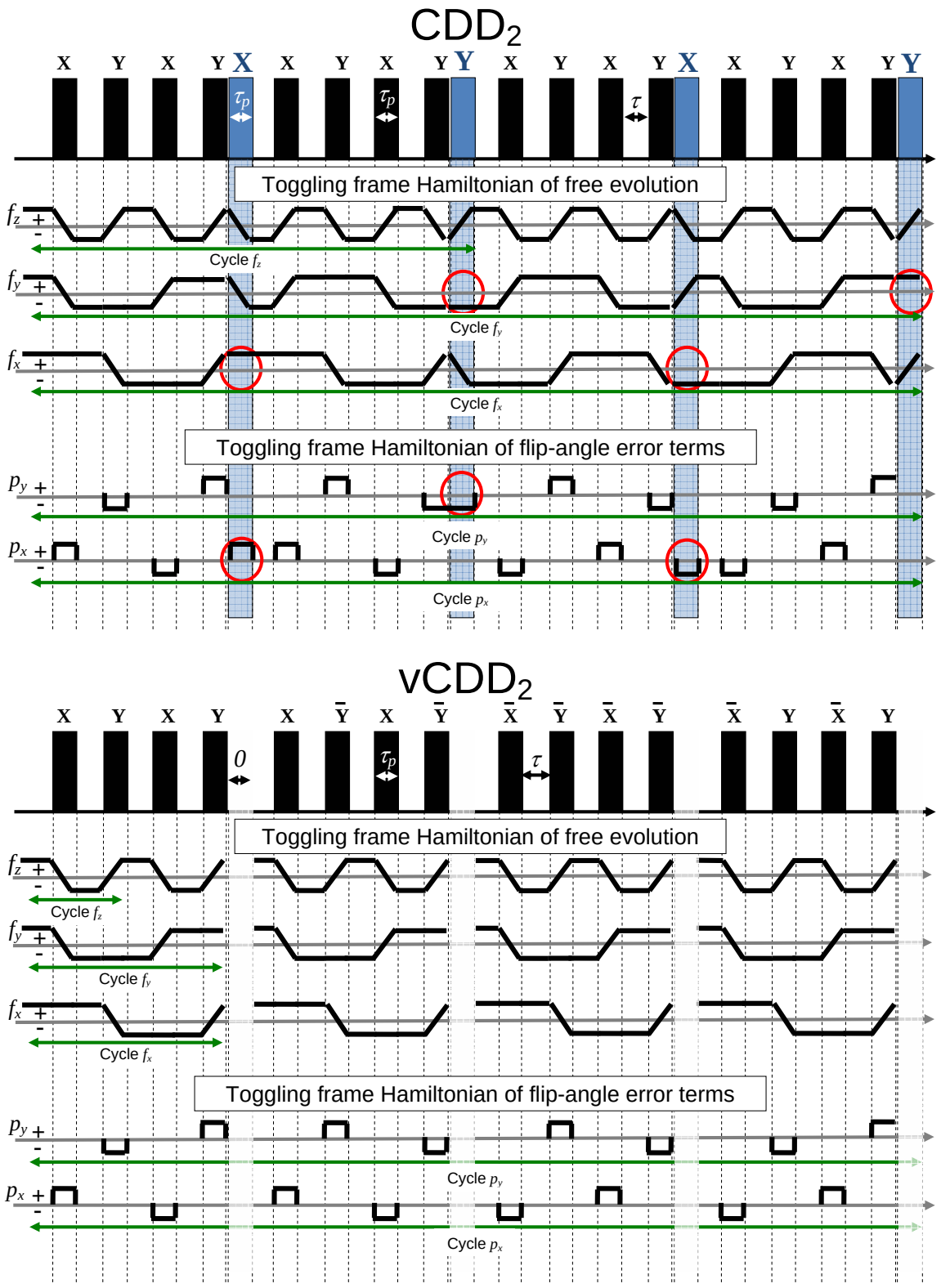

Figure 1: (Color online) CDD_2 and $vCDD_2$ pulse sequence schemes. The black solid boxes represent the DD π-pulses of the inner sequences with their respective phases. The gray (blue) boxes are the π-pulses of the generating sequence for CDD, while for vCDD they are virtual and appear as a transparent white stripe of zero duration. The toggling frame Hamiltonians are represented by the respective signs of the different terms proportional to the $\hat{S}_x$, $\hat{S}_y$ and $\hat{S}_z$ components. Sign changes during the pulses are representedby diagonal lines \ or /. In the CDD_2 scheme, the terms marked by circles are compensated only at the end of the complete cycle, but the vCDD scheme compensates all terms over the basic 4-pulse cycle. The toggling frame Hamiltonians of the free evolution interaction for $vCDD_2$ are the same for all blocks of the inner sequence, i.e., equal to those of the $XY4$ sequence. The toggling frame Hamiltonian of the flip-angle error terms of vCDD is equal to that of the CDD scheme with ideal pulses.

UDD sequences, but the analysis is similar for CDD sequences because the period of the toggling frame sign function f increases with the concatenation order [25].

As shown in Fig. 1, the toggling frame Hamiltonian for one of the components is not affected by the pulses of the generating sequence (marked by circles). Due to the finite duration of the pulses, this represents an additional contribution to the average Hamiltonian, which is only compensated by the second pulse of the generating sequence with the same rotation axis half a period later. Full compensation of these additional terms is achieved at the end of the complete (higher-order) cycle.

Generally more important than their finite duration are imperfections of the pulses. In most cases, the dominant cause of errors is a deviation between the ideal and the actual amplitude of the control fields. This results in a rotation angle that deviates from π, typically by a few percent. The propagator for the π pulses including this error is $e^{-i(\pi+\Delta\omega_p\tau_p)\hat{S}_\phi}$, where $\Delta\omega_p$ is the error on the control field amplitude. In the toggling frame Hamiltonian, the ideal part of this propgator, $e^{-i\pi\hat{S}_\phi}$, vanishes, but the error term $e^{-i\Delta\omega_p\tau_p\hat{S}_\phi}$ remains and contributes to the average Hamiltonian. The signs of these terms in the toggling frame are represented as p_u in Fig. 1.

Another important error occurs when the control field is not applied on resonance with the transition frequency of the qubit. This off-resonance error adds a term $f_z\Delta_z\hat{S}_z$ to the toggling-frame Hamiltonian.

The $XY4$ sequence cancels these errors in zeroth order), independent of the initial condition [48, 50]. As a result, the performance of this sequence is quite symmetric with respect to the initial state in the xy-plane and the average decay times are significantly longer than with non-robust sequences [20, 24, 26, 35]. The concatenation scheme proposed by Khodjasteh and Lidar [5, 33] improves the decoupling performance and the tolerance to pulse imperfections [20, 26]. However, the finite duration of the pulses and constrained delays between pulses result in the existence of optimal levels of concatenation [20, 26], with decreasing performance for higher level sequences. This can be seen in Fig. 2, where decay curves are ploted for different DD sequences, including the free evolution decay, the Hahn echo decay [51] and different orders of CDD for their optimal delay between pulses. Panel b shows the decay times for different CDD sequences and delays τ between pulses. For each sequence, the decoherence time reaches a maximum; for delays shorter than the optimal value, the pulse errors dominate. The relation between the optimal delay time and the its CDD order is plotted in the inset of Fig. 2b). The experimental dependence agrees remakrably well with the predicted curve [33].

C. CDD with virtual pulses

In Ref. [20], we suggested to improve the concatenation scheme by compensating the pulse errors of the generating sequence (gray (blue) boxes, Fig. 1) before the end of the complete cycle. Looking into the details of the toggling frame Hamiltonians, we can see that at each concatenation level, the $XY4$ generating sequence (gray (blue) boxes on the top panel of Fig. 1) additional pulse errors are introduced that are only compensated at the end of the complete cycle. As a result, the properties of the real CDD sequence deviate strongly from that of the ideal sequence.

Here, we show how these additional pulse errors can be completely avoided by using virtual (and thus ideal) rotations for the generating sequence instead of the real ones. To motivate the idea, we consider the first pulse of the generating sequence and the subsequent pulses of the cycle from the lower order sequence. The corresponding evolution operator can be written

$$\ldots\left(\hat{Y}\hat{X}\hat{Y}\hat{X}\right)\hat{X}\ldots \;=\; \ldots\hat{X}\left(\hat{\bar{Y}}\hat{X}\hat{\bar{Y}}\hat{X}\right)\ldots, \qquad (5)$$

where the pulse sequence is read from right to left. The bar over the X and Y means that the sense of rotation is reversed for those pulses. The second form corresponds to a modified $XY4$ cycle, followed by the π_x pulse of the generating sequence. In the modified cycle, the direction of rotation of the y-pulses has been inverted. We distinguish this modified cycle from the original cycle by writing them as $vC_{n-1}(X,\bar{Y})$ and $vC_{n-1}(X,Y)$, respectively. Similarly, the subsequent cycles become $vC_{n-1}(\bar{X},\bar{Y})$ and $vC_{n-1}(\bar{X},Y)$. As the pulses of the generating sequence are thus moved to the end of the cycle, they cancel and can be omitted completely. In this sense, we have replaced these pulses by "virtual pulses" corresponding to phase changes of the pulses in the inner sequence. The resulting sequence, which is shown in Fig. 1, can be written recursively as

$$\mathrm{vCDD}_1(X,Y) = XY4 \qquad (6)$$

$$\mathrm{vCDD}_n(X,Y) = vC_n(X,Y) = vC_{n-1}(X,Y)\text{-}vC_{n-1}(X,\bar{Y})\text{-}vC_{n-1}(\bar{X},\bar{Y})\text{-}vC_{n-1}(\bar{X},Y). \qquad (7)$$

Similarly we can obtain its time-symmetric version.

As shown in Fig. 1, the toggling frame Hamiltonian generated by this sequence differs from that of the original CDD sequence. As shown in the lower part of the figure, the function f has for each 4-pulse block the same time dependence as for the $XY4$ sequence. The terms marked by circles in the upper part of the figure are missing in the lower part; accordingly, the average of the f_u vanishes over each block of the inner sequence. Similarly, the pulse error contributions p_u do not have contributions from the generating sequence and therefore also compensate over each lower order cycle. In lowest order average Hamiltonian, the vCDD sequences therefore compensate all errors over a single $XY4$ cycle, while the corresponding time for CDD_N is 4^N times longer. For the vCDD

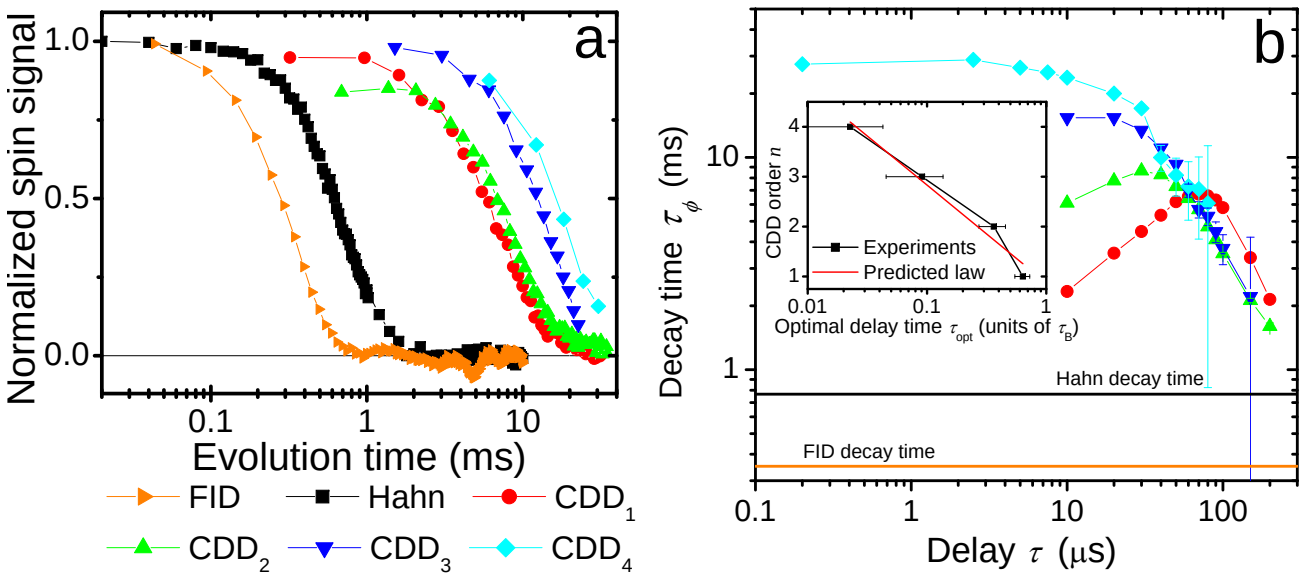

Figure 2: (Color online) Decays of coherence under the influence of different DD sequences. (a) Normalized spin-signal decay of the echo trains of different CDD sequences, the Hahn echo decay [51] and the free evolution (FID). The CDD decay curves are plotted for their optimal delays between pulses that are given when the curves of panel b have a maximum. (b) Decay times of different CDD sequences for different delays between pulses. The optimal delay time is defined when the decay is a maximum. The inset shows its dependence as a function of the CDD order matching with theoretical predictions [33].

sequence, the lowest frequency of the filter function is therefore always $2\pi/\tau_1$, where τ_1 is the duration of the $\mathrm{CDD}_1 = XY4$ cycle. In contrast to that, the fundamental frequency of the CDD_n sequence decreases with $1/4^n$, which can make it sensitive to low-frequency noise with high amplitudes, such as frequency offsets and errors of control fields.

The change in the toggling frame Hamiltonian effected by the pulses of the generating sequence of CDD can of course also be a desired property, since it compensates higher-order terms of the average Hamiltonian, including cross-terms between pulse imperfections and environmental contributions. Some of these effects are also present in the vCDD scheme, since the non-vanishing higher-order average Hamiltonians of the different blocks are not identical. The concatenation scheme is designed to compensate them over the full cycle. A detailed discussion of these higher-order contributions is beyond the scope of this paper and probably not feasible without considering specific system parameters. Instead, we compare the two schemes experimentally.

IV. EXPERIMENTAL PERFORMANCE COMPARISON

A. System and setup

We experimentally implemented the new vCDD scheme and compared its performance to that of the normal CDD scheme. The experiments were performed on a polycrystalline adamantane sample using a home-built solid state NMR spectrometer with a ^{1}H resonance frequency of 300 MHz. Our system qubits are the ^{13}C nuclear spins of the adamantane molecule, which contains two nonequivalent carbon atoms. Under our conditions, they have similar dynamics. Here, we present the results from the CH_2 carbon. Working with a natural abundance sample (1.1 % ^{13}C), the interaction between the ^{13}C-nuclear spins can be neglected. The main mechanism for decoherence is the interaction with the neighboring proton spins. As discussed before, this interaction generates pure dephasing. This interaction is not static, since the dipole-dipole couplings within the proton bath cause flip-flops of the protons coupled to the carbon. The π pulses for DD were applied on resonance with the ^{13}C spins. Their radio-frequency (RF) field of $\approx 2\pi \times 50$ kHz gives a π-pulse length τ_p between 10μs and 10.6μs. The measured RF field inhomogeneity was about 10%.

B. vCDD and CDD under optimal conditions

Figure 3 compares the decay of the spin signal for the asymmetric versions of CDD_2 and vCDD_2 for two different pulse spacings τ. For the vCDD_2-sequence, the decay is clearly slower; the $1/e$ decay times are 17 ms and 14.6 ms for the two delays, compared to 8.9 ms and 10.1 ms for the CDD2 sequence.

Figure 4 shows the decay times for different asymmetric CDD and vCDD orders obtained for different duty cycles, *i.e.*, the ratio between the irradiation time $N_p\tau_p$

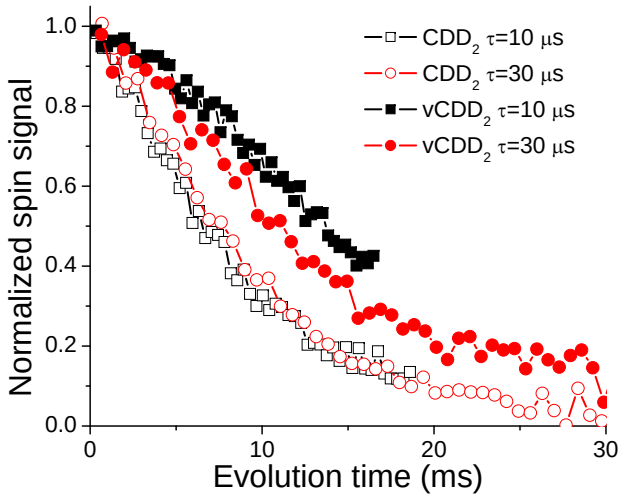

Figure 3: (Color online) Normalized spin signal decays for $vCDD_2$ and CDD_2 for different delays τ .

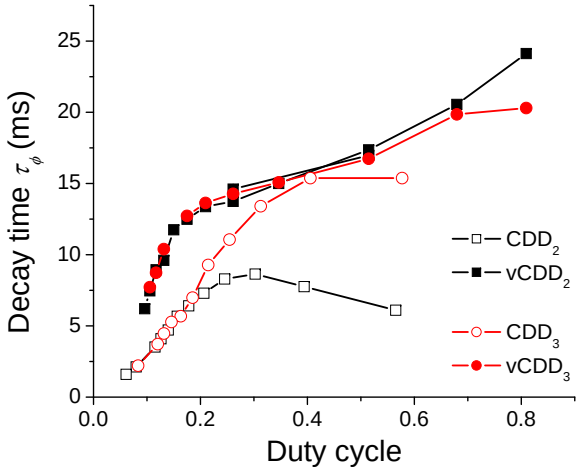

Figure 4: (Color online) Decay times for vCDD and CDD of order 2 and 3 as a function of the duty cycle.

over the total time $(N_p\tau_p + N\tau)$, where N_p is the number of pulses in a cycle and N the number of delays. τ_p was kept fixed and we varied the delay τ between the pulses. Comparing the curves for the two schemes, we find that vCDD performs better than the CDD sequences for all duty cycles (delays). While the CDD performance changes as a function of the order, the difference between the two vCDD sequences is not significant. The difference beween the symmetric and asymmetric version of vCDD also was not significant. This suggests that the 2^{nd} order achieves already the optimal DD performance for our experimental conditions. The observed performance is also very similar to that of the KDD sequence measured in an earlier study (see Ref. [26] for details). Both, the vCDD and the CDD sequences perform symmetrically for initial conditions in the xy-plane.

C. Effect of pulse errors

Under normal experimental conditions, we cannot see any difference between the vCDD scheme and other robust sequences like KDD and $XY16$ [20, 26, 35, 41]. To quantitate this robustness we also tested the performance of the sequence against artificially added pulse errors. We compared CDD with vCDD and with the optimal sequences obtained in previous works, *i.e.*, $XY16$ and KDD [26, 35, 41]. Figures 5 and 6 compare the spin signal after one cycle of the respective sequence for different pulse errors. Fig. 5 shows the surviving spin polarization as a function of the pulse duration (and thus of the flip angle) and the delay between the pulses. The number of pulses per cycle is not exactly the same for the different sequences (16 for $vCDD_2$ and $XY16$ vs. 20 for CDD_2 and KDD), but we consider this to be sufficiently similar to allow a rough comparison. For all sequences, there is little correlation between the flip angle error and the delay between the pulses. This is a consequence of the fact that the terms in the propagator that involve the flip-angle error are proportional to the pulse width τ_p but independent of the pulse separation τ.

Figure 6 shows similar data, but here we introduced an artificial offset error Δ_z rather than a flip-angle error. In this case, there is a strong correlation between the effect of the offset and the delay between the pulses. This is expected, because an offset error generates an extra dephasing term in the propagator that generates an additional precession by an angle $\Delta_z\tau$. Without the SE interaction or another source of errors (like flip-angle error inhomogenity), we do not expect a significant dependence on τ, because the offset is static and can be completly refocused with DD. Our real system has a bath correlation time of ≈ 100 μs [20, 25], which explains the observed decay for cycle times of this order.

Comparing the standard CDD_2 with the symmetric version of $vCDD_2$ in Fig. 5a,b, we can see that the overall performance of vCDD is better than that of CDD, as expected by the analysis of section III. This is because vCDD is more effective in compensating the flip-angle errors. vCDD also outperforms CDD in the presence of offset errors (see Fig. 6a,b). Comparing the asymmetric and symmetric version of vCDD as a function of flip angle error, we observe no significant differences. However, vCDD(s) clearly outperfroms vCDD(a) in the presence of offset errors (Fig. 7). Comparing against the other sequences, $vCDD_2$ seems to perform better than KDD as a function of flip-angle errors. The good performance of $XY16$ is expected because its evolution operators (symmetric and asymmetric) are equal to the identity operator as long as spin-bath effects are absent: the sequence is designed to generate a propagator $U\,U^{\dagger}$, independent of flip-angle errors. For small delays between pulses, $XY16$ is the most robust sequence as a function of flip-angle error. Its symmetric version performs slightly better than the asymmetric version. As a function of offset error, $vCDD_2$(s), KDD and $XY16$(s) behave similarly and they

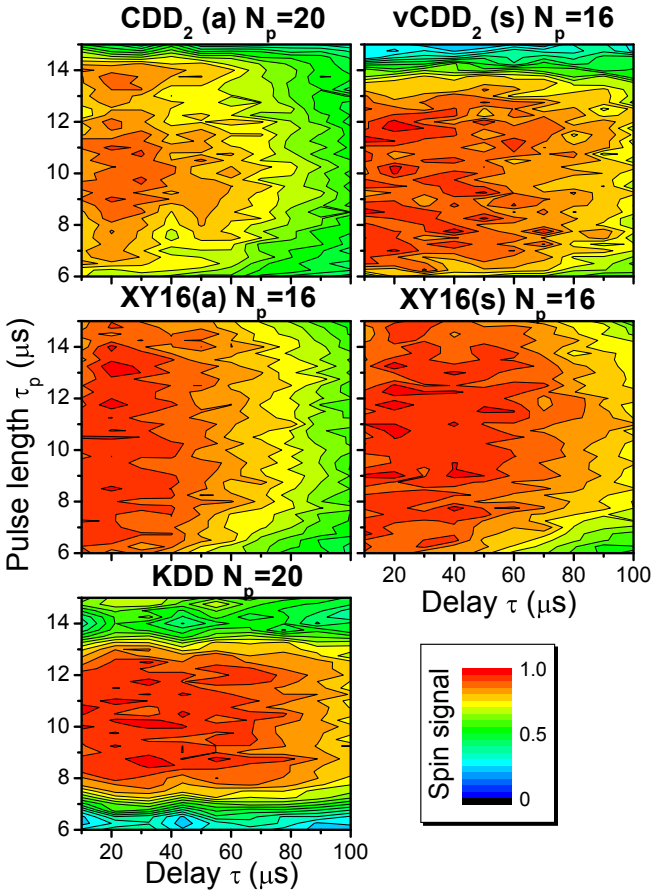

Figure 5: (Color online) Normalized spin-signal after 1 cycle of different DD sequences as a function of the pulse-length of the DD pulses and the delay between them. The labels (a) and (s) refers the the asymmetric and symmetric version of the sequences.

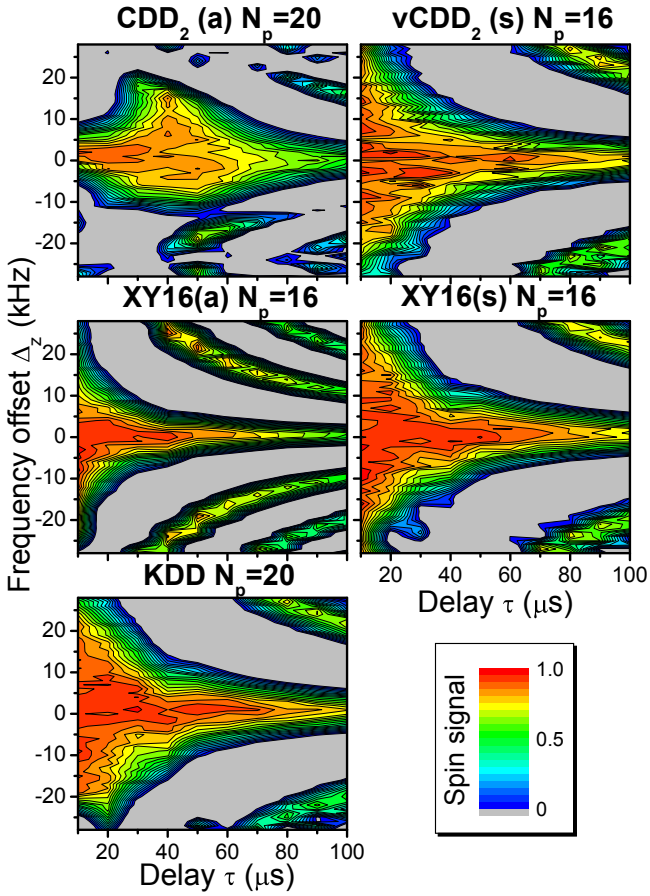

Figure 6: (Color online) Normalized spin-signal after 1 cycle of different DD sequences as a function of the RF pulse frequency of the DD pulses and the delay between them. The labels (a) and (s) refers the the asymmetric and symmetric version of the sequences.

are more robust than vCDD$_2$(a) and $XY16$(a). Note that the behaviour of the asymmetric version of vCDD$_2$ and $XY16$ as a function of offset errors are also similar.

To amplify the effect of pulse imperfections, we also performed experiments with ≈100 pulses as a function of the delay between the pulses and added specific pulse imperfections (Figs. 8 and 9). Under these conditions, also the accumulated exposure to the spin-bath is longer. Cleary now the vCDD sequence outperforms always the CDD version for every condition. As a function of flip angle error, the performance of vCDD(s) and vCDD(a) is comparable (vCDD(a) is not shown). The vCDD perfomance as a function of flip angle error is even better than KDD and comparable to the $XY16$(s) . As a function of offset error, the performance of vCDD$_2$(s) is comparable to KDD and $XY16$(s); however in this case vCDD$_2$(a) is less robust (not shown in the figure).

V. OTHER GENERATING SEQUENCES

The concept introduced here can can not only be applied to the $XY4$ sequence but also to other generating sequences, such as the KDD sequence [26]. KDD was inspired from a sequence of adjacent π pulses that combine to a robust π pulse [52]

$$\Pi_\phi = \pi_{\phi+30} - \pi_{\phi+0} - \pi_{\phi+90} - \pi_{\phi+0} - \pi_{\phi+30}. \qquad (8)$$

The decoupling sequence is obtained first by introducing delays between the individual pulses: [26]

$$\Pi_\phi(\tau) = \pi_{\phi+30}\text{-}f_\tau\text{-}\pi_{\phi+0}\text{-}f_\tau\text{-}\pi_{\phi+90}\text{-}f_\tau\text{-}\pi_{\phi+0}\text{-}f_\tau\text{-}\pi_{\phi+30}. \qquad (9)$$

The lower indexes denote the pulse phase, i.e. the orientation of the rotation axis in the xy-plane. If we use $XY4$ as the (virtual) generating sequence and $\Pi_\phi(\tau)$ as building blocks, we arrive at

$$\text{KDD} = \Pi_X(\tau) - \Pi_Y(\tau) - \Pi_X(\tau) - \Pi_Y(\tau), \qquad (10)$$

which we introduced and tested in [26].

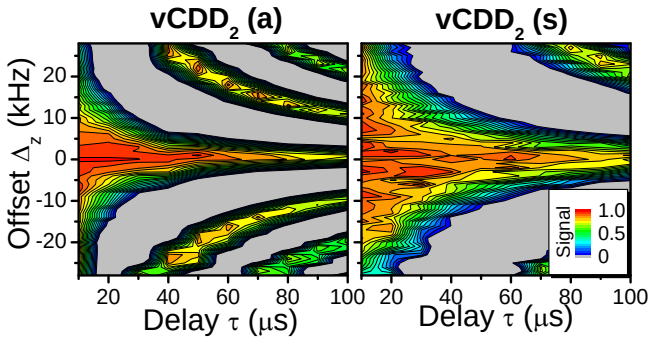

Figure 7: (Color online) Normalized spin-signal after 1 cycle for the symmetric (s) and asymmetric (a) version of vCDD$_2$ as a function of the offset frequency of RF pulse of the DD pulses and the delay between them. Both sequences have the same number of pulses and cycle time.

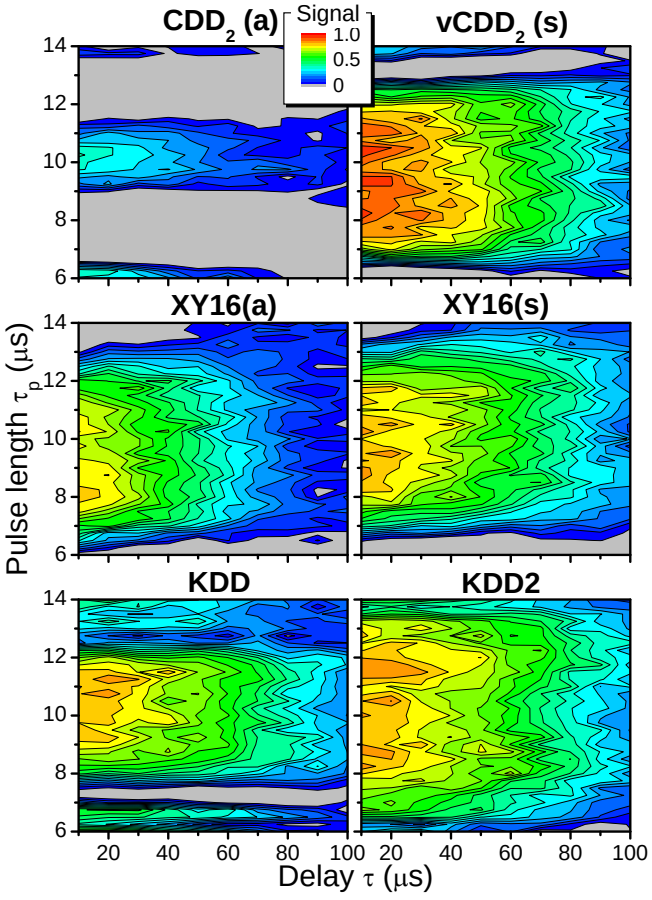

Figure 8: (Color online) Normalized spin-signal after about 100 pulses for different DD sequences as a function of the pulse-length of the DD pulses and the delay between them. All sequences have 100 pulses except vCDD$_2$, which contains 96. The labels (a) and (s) refers the the asymmetric and symmetric version of the sequences.

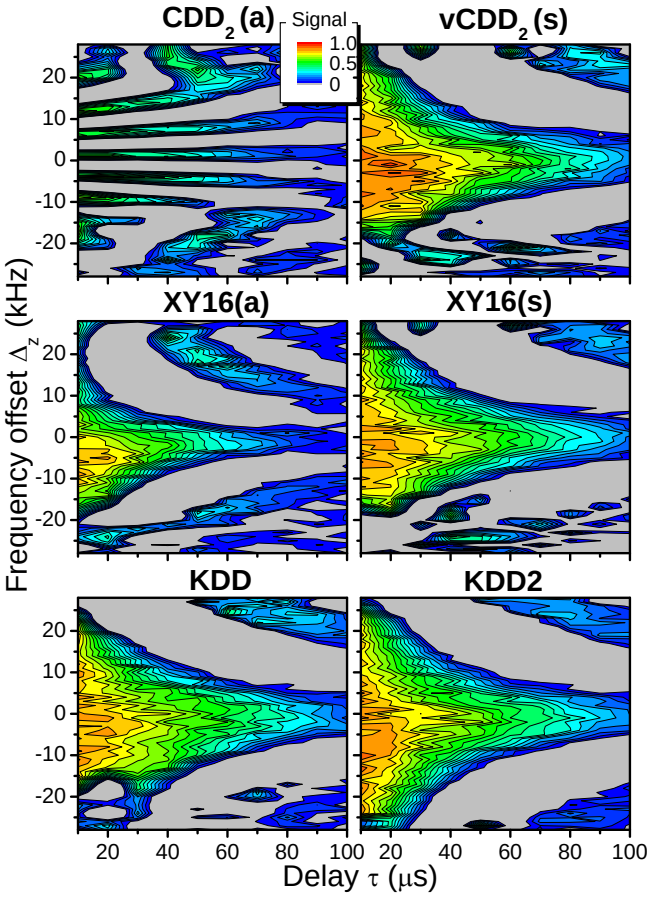

Figure 9: (Color online) Normalized spin-signal after about 100 pulses for different DD sequences as a function of the RF frequency of the DD pulses and the delay between them. All sequences have 100 pulses except vCDD$_2$, which contains 96. The labels (a) and (s) refers the the asymmetric and symmetric version of the sequences.

If we use the sequence (8) instead of $XY4$ as the (virtual) generating sequence, we obtain a new sequence

$$\mathrm{KDD2} = [\Pi_{30}(\tau) - \Pi_0(\tau) - \Pi_{90}(\tau) - \Pi_0(\tau) - \Pi_{30}(\tau)]^2 .$$

As indicated by the square after the bracket, the complete cycle consists of 50 pulses. Iterations to higher order are of course possible but will not be covered here.

In Fig. 8 and 9, we also show the experimental performance of this new sequence, together with the sequences discussed earlier. We clearly see that this new sequene is extremely robust and outperfoms all other sequences.

VI. CONCLUSIONS

We have presented a novel method for concatenated dynamical decoupling: for the generating sequence, we use virtual rotations instead of physical control operations. Since these rotations are ideal, our new scheme

avoids introducing additional pulse imperfections, reduces the power deposition on the system and makes the resulting sequences more robust. As a result of the reduced number of control operations, the toggling frame Hamiltonian has a different time dependence than in the standard CDD scheme. We have tested two different expansion schemes based on these virtual rotations, called vCDD and KDD2. Both types of sequences have proved to be very robust under our experimental conditions. It will be interestig to see if these results can be reproduced in other systems.

Acknowledgments

Acknowledgments.—We aknowledge discussion with Daniel Lidar and Gregory Quiroz. This work is supported by the DFG through Su 192/24-1.

[1] T. D. Ladd, F. Jelezko, R. Laflamme, Y. Nakamura, C. Monroe, and J. L. O'Brien, Nature **464**, 45 (2010).
[2] W. Zurek, Rev. Mod. Phys. **75**, 715 (2003).
[3] L. Viola, E. Knill, and S. Lloyd, Phys. Rev. Lett. **82**, 2417 (1999).
[4] L. Viola and E. Knill, Phys. Rev. Lett. **90**, 037901 (2003).
[5] K. Khodjasteh and D. A. Lidar, Phys. Rev. Lett. **95**, 180501 (2005).
[6] G. S. Uhrig, Phys. Rev. Lett. **98**, 100504 (2007).
[7] G. Gordon, G. Kurizki, and D. A. Lidar, Phys. Rev. Lett. **101**, 010403 (2008).
[8] G. S. Uhrig, Phys. Rev. Lett. **102**, 120502 (2009).
[9] J. R. West, B. H. Fong, and D. A. Lidar, Phys. Rev. Lett. **104**, 130501 (2010).
[10] K. Khodjasteh, D. A. Lidar, and L. Viola, Phys. Rev. Lett. **104**, 090501 (2010).
[11] J. Clausen, G. Bensky, and G. Kurizki, Phys. Rev. Lett. **104**, 040401 (2010).
[12] W. Yang, Z. Wang, and R. Liu, Front. Phys. **6**, 2 (2010).
[13] Z. Wang and R. Liu, Phys. Rev. A **83**, 022306 (2011).
[14] G. Quiroz and D. A. Lidar, Phys. Rev. A **84**, 042328 (2011).
[15] W. Kuo and D. A. Lidar, Phys. Rev. A **84**, 042329 (2011).
[16] L. Cywinski, R. M. Lutchyn, C. P. Nave, and S. Das-Sarma, Phys. Rev. B **77**, 174509 (2008).
[17] W. Yang and R. Liu, Phys. Rev. Lett. **101**, 180403 (2008).
[18] M. J. Biercuk, *et al.*, Nature **458**, 996 (2009).
[19] J. Du, *et al.*, Nature **461**, 1265 (2009).
[20] G. A. Álvarez, A. Ajoy, X. Peng, and D. Suter, Phys. Rev. A **82**, 042306 (2010).
[21] G. de Lange, Z. H. Wang, D. Riste, V. V. Dobrovitski, and R. Hanson, Science **330**, 60 (2010).
[22] C. Barthel, J. Medford, C. M. Marcus, M. P. Hanson, and A. C. Gossard, Phys. Rev. Lett. **105**, 266808 (2010).
[23] S. Pasini and G. S. Uhrig, Phys. Rev. A **81**, 012309 (2010).
[24] C. A. Ryan, J. S. Hodges, and D. G. Cory, Phys. Rev. Lett. **105**, 200402 (2010).
[25] A. Ajoy, G. A. Álvarez, and D. Suter, Phys. Rev. A **83**, 032303 (2011).
[26] A. M. Souza, G. A. Álvarez, and D. Suter, Phys. Rev. Lett. **106**, 240501 (2011).
[27] I. Almog, Y. Sagi, G. Gordon, G. Bensky, G. Kurizki, and N. Davidson, J. Phys. B: At., Mol. Opt. Phys. **44**, 154006 (2011).
[28] B. R. Bardhan, P. M. Anisimov, M. K. Gupta, N. C. Jones, H. Lee, and J. P. Dowling, arXiv:1105.4164 (2011).
[29] Y. Pan, Z. Xi, and J. Gong, J. Phys. B: At., Mol. Opt. Phys. **44**, 175501 (2011).
[30] A. Shukla and T. S. Mahesh, arXiv:1110.1473 (2011).
[31] H. Bluhm, S. Foletti, I. Neder, M. Rudner, D. Mahalu, V. Umansky, and A. Yacoby, Nat. Phys. **7**, 109 (2011).
[32] B. Naydenov, F. Dolde, L. T. Hall, C. Shin, H. Fedder, L. C. L. Hollenberg, F. Jelezko, and J. Wrachtrup, Phys. Rev. B **83**, 081201 (2011).
[33] K. Khodjasteh and D. A. Lidar, Phys. Rev. A **75**, 062310 (2007).
[34] T. E. Hodgson, L. Viola, and I. D'Amico, Phys. Rev. A **81**, 062321 (2010).
[35] A. M. Souza, G. A. Álvarez, and D. Suter, accepted in Phil. Trans. R. Soc. A (2012), arXiv:1110.6334 (2011).
[36] Z. Wang and V. V. Dobrovitski, J. Phys. B: At., Mol. Opt. Phys. **44**, 154004 (2011).
[37] Z. Xiao, L. He, and W.-g. Wang, Phys. Rev. A **83**, 032322 (2011).
[38] Z. Wang, W. Zhang, A. M. Tyryshkin, S. A. Lyon, J. W. Ager, E. E. Haller, and V. V. Dobrovitski, arXiv:1011.6417 (2010).
[39] K. Khodjasteh, T. Erdélyi, and L. Viola, Phys. Rev. A **83**, 020305 (2011).
[40] X. Peng, D. Suter, and D. A. Lidar, J. Phys. B: At., Mol. Opt. Phys. **44**, 154003 (2011).
[41] A. M. Souza, G. A. Álvarez, and D. Suter, accepted in Phys. Rev. A (2012), arXiv:1110.1011 (2011).
[42] J. M. Cai, F. Jelezko, M. B. Plenio, and A. Retzker, arXiv:1111.0930 (2011).
[43] A. Abragam, *Principles of Nuclear Magnetism* (Oxford University Press, London, 1961).
[44] H. Y. Carr and E. M. Purcell, Phys. Rev. **94**, 630 (1954).
[45] S. Meiboom and D. Gill, Rev. Sci. Instrum. **29**, 688 (1958).
[46] R. Hanson, *et al.*, Rev. Mod. Phys. **79**, 1217 (2007).
[47] B. E. Kane, Nature **393**, 133 (1998).
[48] A. A. Maudsley, J. Magn. Reson. **69**, 488 (1986).
[49] G. A. Álvarez and D. Suter, Phys. Rev. Lett. **107**, 230501 (2011).
[50] T. Gullion, D. B. Baker, and M. S. Conradi, J. Magn. Reson. **89**, 479 (1990).
[51] E. L. Hahn, Phys. Rev. **80**, 580 (1950).
[52] R. Tycko, A. Pines, and J. Guckenheimer, J. Chem. Phys. **83**, 2775 (1985).